Comparison between two tailored press hardening technologies by means of physical and numerical simulation

Maria Emanuela Palmieri[1,a *], Luigi Tricarico[1,b]

[1]Department of Mechanical Engineering, Mathematics & Management Engineering, Politecnico of Bari, Via Orabona, 4, 70125 Bari, Italy

[a]mariaemanuela.palmieri@poliba.it, [b]luigi.tricarico@poliba.it

Keywords: Sheet Forming, Automotive, Tailored Properties

Abstract. Tailored Tool Tempering (TTT) and Intermediate Pre-Cooling techniques are two tailored press hardening technologies studied for automotive applications to obtain structural components with good energy absorption characteristics and high strength. The aim of this work is the comparison between these two tailored technologies in terms of mechanical properties on the part. An automotive B-Pillar in 22MnB5 steel was considered as case study. Two Finite Element (FE) models were developed for simulating both technologies. FE thermal cycles were experimentally reproduced on specimens using a Gleeble physical simulator. After physical simulation, metallographic, tensile and hardness tests were carried out to evaluate the mechanical properties. Optimal values of process parameters that guarantee ductile and resistant zones on the same component were detected. In these optimal conditions, the TTT technology guarantees greater fracture deformability in the component zone which is to absorb energy.

Introduction

The reduction of fuel consumption and the improvement of safety for passengers are the main objectives for transport industries [1]. To fulfill these objectives, for several decades, the focus is on reducing the vehicle structures mass and optimizing production processes [2]. The trend to reduce vehicle weight was further increased due to the production of electric vehicles, where the battery mass should be compensated [3]. Ultra-strength materials such as advanced high-strength boron steels and the press hardening process promote the reduction of vehicle body structures mass [1]. The press hardening process is a combination of two operations, namely, the hot forming of a fully austenitized blank in a furnace at about 900 °C and the quenching heat treatment in the forming tools that leads to a martensitic microstructure on the component [1]. This technology is well suited for the production of components with diversified mechanical properties (tailored components) [4], in order to simultaneously guarantee high impact resistance and good energy absorption capacity. These components can be produced either by tailored blank technologies or by tailored process technologies [1]. The tailored blank technologies include: Tailored Rolled Blanks (TRB) [5], Tailored Welded Blanks (TWB) [6] and Patchwork blanks [7]. Tailored process technologies, on the other hand, allow to obtain components with customized mechanical properties by modifying microstructural properties of the part through heat treatments after the press hardening process or through the variation of thermal cycles (modification of the press hardening process). Some examples of tailored process technologies are detailed below: laser partial annealing [8], Tailored Blank Heating (TBH), known also as partial heating [4], Tailored Tool Tempering (TTT) and the relatively recent Intermediate Pre-Cooling (IPC). In this work the attention is focused on the TTT and the IPC technologies. The first one involves the use of tools with heated segments (by means of cartridge heaters) in areas where a ductile area should be generated and cooled segments (by means of cooling channels) where resistant regions are desired [9]. This technology is also known in the literature as differential cooling [4]. The second one uses, downstream to the conventional austenitizing furnace, an additional furnace (tempering station), where selected blank regions are cooled to guarantee the required part ductility while the other blank areas are maintained at the austenitization temperature [10]. This new technology differs from the conventional partial heating technology since the temperature partitioning of the blank takes place after the complete autenitization phase. The TTT technology is better described in Fig. 1, where the scheme of the process (Fig. 1a) and of the thermal cycles (Fig. 1b) are shown in correspondence of resistant and ductile regions. In Fig. 1b, the solid orange curve represents the thermal cycle of the ductile region, while the dashed blue curve represents the thermal cycle of the resistant region. During the quenching phase, the high cooling rates in the resistant regions of the component lead to a martensitic microstructure at the end of the process. Conversely, lower cooling rates lead to more ductile microstructures, e.g., bainitic microstructure. Several scientific works showed that the microstructure and mechanical properties of the part in the ductile region is mainly influenced by the temperature of heated tools and the quenching time in the tools [11]. The IPC technology and resulting thermal cycles in ductile and resistant regions are schematized in Fig. 2. Specifically, from Fig. 2a it can be seen that the blank is first austenitized in the furnace and then it is moved into a second furnace where the intermediate pre-cooling is obtained by masking the blank regions which define the ductile area of the part. The masked areas are cooled below approximately 700 °C, while the unmasked areas are reheated to about 950 °C (austenitization temperature). This solution was patented by the AP&T Company with the TemperBox® tempering furnace [12]. In Fig. 2b, the thermal cycle of the ductile region is represented with the solid orange line, while the thermal cycle of the resistant region is represented with the dashed blue line. The slow cooling in the tempering station in correspondence of the masked areas leads to a predominantly ferritic-pearlitic microstructure that confers ductility properties to these areas. This latter technology is quite recent, therefore still few works studied it. Moreover, for the best authors knowledge, nobody compared yet these two investigated technologies which lead to different microstructures in the soft region. The objective of this work is to compare the TTT technology with the new IPC technology in terms of mechanical properties of the part at the end of the process, after evaluating the influence of the process parameters for both technologies. For the TTT technology, the process parameters evaluated were the temperature of the heated tools (T_q) and the quenching time in the tools (t_q). Instead, for the IPC technology, the parameters considered were the time taken in the tempering station ($t_{precooling}$) and the temperature to which the blank drops in correspondence with the ductile regions ($T_{precooling}$).

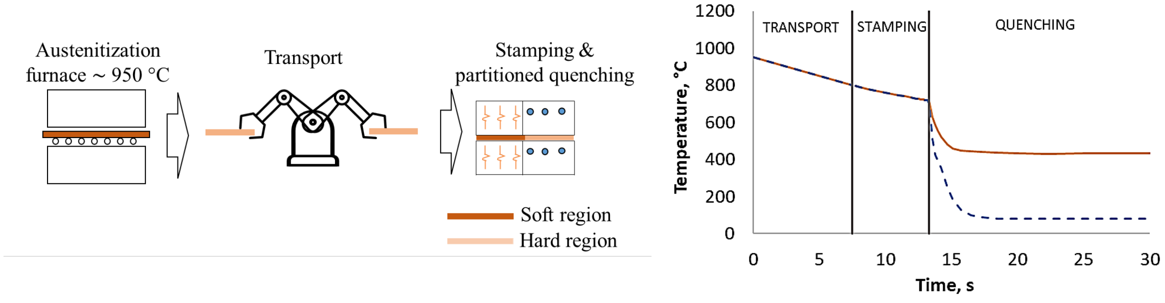

(a) (b)

Fig. 1. Press hardening with tailored tool tempering approach (a) scheme of the process and (b) scheme of thermal cycles in ductile and resistant regions.

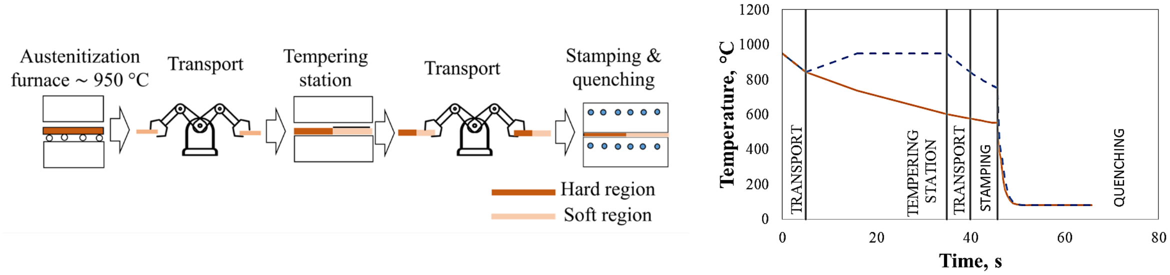

(a) (b)

Fig. 2. Press hardening with intermediate pre-cooling approach (a) scheme of the process and (b) scheme of thermal cycles in ductile and resistant regions.

Materials and Method

In order to compare the two investigated tailored technologies, an automotive structural component was chosen as a case study, i.e., the B-Pillar shown in Fig. 3, manufactured starting from a 1.3 mm thick blank in 22MnB5 steel (C=0.217 %, Mn=1.16 % and B=0.0029 %). As can be seen in Fig. 3, a more strength central area and two more ductile areas (lateral ones) are required for this component. The study was carried out by means of physical and numerical simulations. First, using the Finite Element (FE) commercial software, AutoForm®R10, two FE models were developed; one allows the numerical simulation of the press hardening process with the tailored tool tempering technology, the other, the numerical simulation of the intermediate pre-cooling technology. The numerical simulations were performed varying the process parameters (t_q and T_q for the TTT technology and $t_{precooling}$ and $T_{precooling}$ for the IPC technology). The numerical simulations were set as in Tab. 1 for the TTT technology and as in Tab. 2 for the IPC technology. The ranges of process parameters were identified based on previous studies [9, 13].

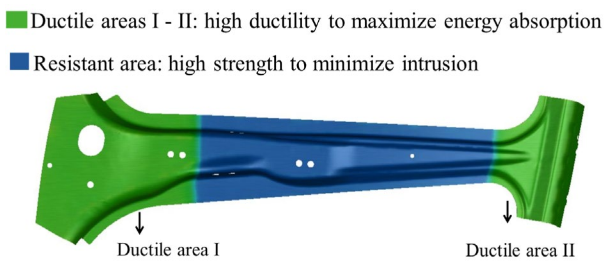

Fig. 3. Case study: B-Pillar with one central resistant area and two lateral ductile areas

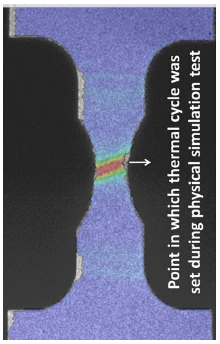

Fig. 4. Notched specimen for tensile testing.

Tab. 1. FE simulations plan for TTT technology.

T_q, °C	t_q, s
430	5-20-35-50
465	5-20-35-50
500	5-20-35-50

Tab. 2. FE simulations plan for IPC technology.

$T_{precooling}$, °C	$t_{precooling}$, s
600	30-90-150-210
650	30-90-150-210
700	30-90-150-210

Both FE models take into account the influence of the temperature and the strain rate on the flow stress and phase transformations. Specifically, the flow curves of the 22MnB5 steel are defined for different microstructural phases (austenite, ferrite-pearlite, bainite and martensite), for a temperature between 20 °C and 850 °C and a strain rate between 0.01 s^{-1} and 1 s^{-1}. For estimating microstructural phases and hardness on the component, in both FE models the continuous cooling transformation phase diagram (CCT) and the steel composition were defined. The heat transfer coefficient (HTC) between blank and ambient was set equal to 0.02 mW/(mm^{2}K) for a temperature of 20 °C and equal to 0.075 mW/(mm^{2}K) for a temperature of 950 °C. Instead, the HTC between blank and tools was defined as a function of the contact pressure and the gap between blank and tools. For the lubrication conditions the Coulomb model was used and a friction coefficient equal to 0.4 was set. Finally, Elastic Plastic Shell (EPS) elements were adopted for the numerical simulations.

At the end of numerical simulations, for both technologies, the numerical hardness values and the predicted microstructure were evaluated. Moreover, the thermal cycles in the resistant area and in one of the two ductile areas (area II) were extracted. The numerical thermal cycles were then physically simulated on 1.3 mm thick 22MnB5 steel specimens, using the Gleeble®3180 system. The physically simulated specimens were then subjected to Vickers hardness tests (load 10 kg and dwell time 10 s), metallographic analyses (after etching with 2 % nital solution), and tensile tests. The tensile tests were assisted by a Digital Image Correlation (DIC) system in order to acquire the mechanical behaviour in the specimen centre where the thermal cycle was set during physical simulation test. To allow the localization of the deformation at this point, as can be seen from Fig. 4, the specimens were notched.

Results and discussion

The numerical simulations results show that in the resistant area, regardless of the process parameters values, a completely martensitic microstructure is estimated with an average hardness of 490 HV10. This is valid for both investigated technologies. In the ductile areas, on the other hand, the microstructure and the hardness are significantly influenced by the process parameters. Some FE results in terms of microstructural phases at the end of the process are reported in Fig. 5 for the TTT technology and in Fig. 6 for the IPC technology.

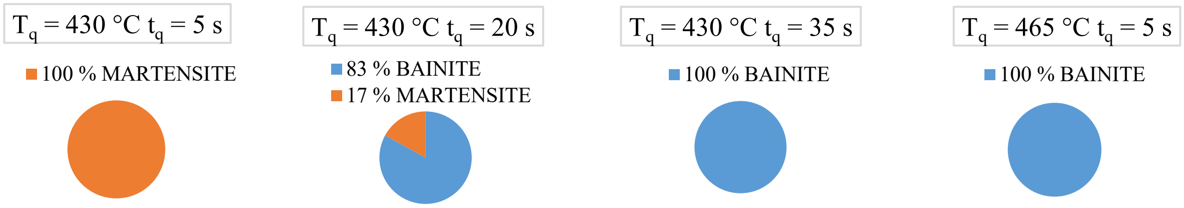

(a) (b) (c) (d)

Fig. 5. Pie chart of the microstructure in the ductile area of the component at the end of the press hardening process with TTT technology as the parameters T_q and t_q vary: (a) T_q = 430 °C – t_q = 5 s; (b) T_q = 430 °C – t_q = 20 s; (c) T_q = 430 °C – t_q = 35 s; (d) T_q = 465 °C – t_q = 5 s.

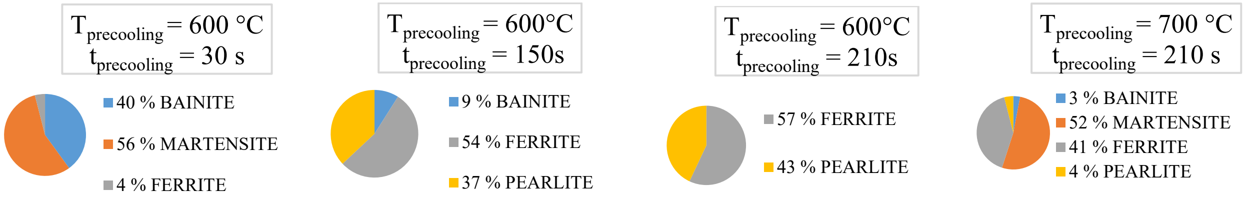

(a) (b) (c) (d)

Fig. 6. Pie chart of the microstructure in the ductile area of the component at the end of the press hardening process with IPC technology as the parameters $T_{precooling}$ and $t_{precooling}$ vary: (a) $T_{precooling}$ = 600 °C – $t_{precoling}$ = 30 s; (b) $T_{precooling}$ = 600 °C – $t_{precoling}$ = 150 s; (c) $T_{precooling}$ = 600 °C – $t_{precoling}$ = 210 s; (d) $T_{precooling}$ = 700 °C – $t_{precoling}$ = 210 s.

Fig. 5 shows that at low temperatures (T_q = 430 °C) as the quenching time increases, the fraction of bainite (more ductile microstructural phase respect to the martensite microstructure) increases. For T_q equal to 430 °C, the complete bainitic transformation is reached for t_q equal to 35 s. At high temperatures (T_q = 465 °C - 500 °C), instead, a quenching time of 5 s is sufficient to complete the bainitic transformation. Fig. 6, on the other hand, shows that as $t_{precooling}$ increases, the percentage of more ductile microstructures (ferrite and pearlite) increases. However, at high temperatures ($T_{precooling}$ = 700 °C), even for the greater $t_{precooling}$ a certain percentage of the harder martensite microstructure is always estimated.

Consistent with the microstructural results, the FE hardness results in the ductile area show that in the TTT technology an increase in the heated tools temperature and in the quenching time lead to a reduction in hardness. For a fixed value of the heated tool temperature, there is a threshold value of the quenching time such that the complete bainitic transformation is obtained and the hardness value remains constant. This threshold value is equal to 35 s for T_q = 430 °C.

Meanwhile, FE hardness results in the ductile area of the component stamped with the IPC technology show that the hardness decreases as the $T_{precooling}$ decreases and $t_{precooling}$ increases.

Such FE hardness results are shown in Fig. 7 (Fig. 7a for TTT technology and Fig. 7b for IPC technology). Fig. 7a shows that the minimum hardness condition for TTT technology is reached for T_q = 500 °C already for t_q = 5 s. Instead, in the IPC technology the minimum hardness condition is obtained for $T_{precooling}$ = 600 °C and $t_{precooling}$ = 210 s. Under these conditions of maximum softening (i.e., minimum hardness), comparing the two technologies, it can be derived that for the IPC approach, in the ductile region, the hardness is approximately 40 % lower than that achieved in the TTT approach.

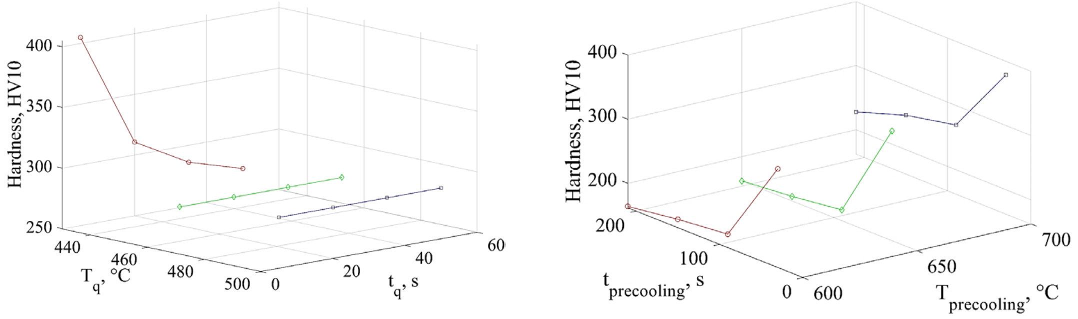

(a) (b)

Fig. 7. FE hardness results as a function of process parameters for (a) the TTT technology and (b) the IPC technology.

As described in the methodology section, the numerical results were then validated through experimental tests. From the hardness and metallographic analyses on specimens subjected to the thermal cycles of the TTT technology, a good agreement with the numerical results was found. Specifically, the experimental hardness values differ of about 2 % from the FE data. Furthermore, metallographic analyses confirm a completely martensitic microstructure in the resistant area for each value of the T_q and t_q, and a predominantly bainitic microstructure in the ductile area already for T_q = 465 °C and t_q = 5s (Fig. 8).

The results of hardness tests on specimens subjected to the thermal cycles of the IPC technology show a good agreement with the numerical predictions only in the ductile area (error percentage of about 5 %). In the resistant area, instead, the experimental hardness shows a decreasing trend as the time taken in the tempering station increases. As an example, Fig. 9 shows the results for $T_{preccoling}$ = 600°C. This reduction in hardness is justified by the grain growth that occurs when the material is heated at high temperature for long time. The grain growth is confirmed by comparing the microstructure obtained for a $t_{precooling}$ = 30 s (image on the left in Fig. 9) with the one obtained for $t_{precooling}$ = 210 s (image on the right in Fig. 9). A martensitic microstrucutre is observed in both figures, however in the microstructure for the lower value of $t_{precooling}$ the size of the lath martensite is smaller than that in the microstructure observed for the greater value of $t_{precooling}$.

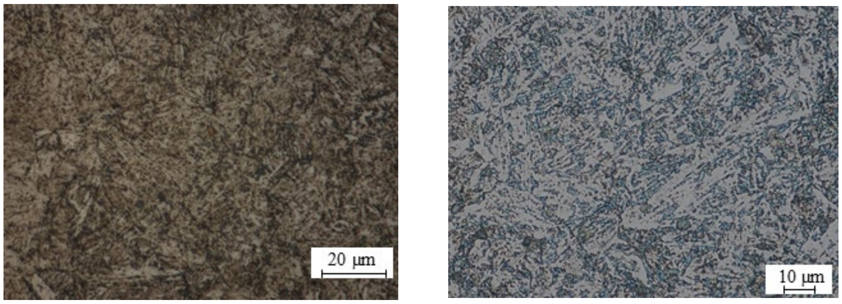

(a) (b)

Fig. 8. Micrographs (1000X) corresponding to the thermal cycles of the resistant area (a) and ductile area (b) for T_q equal to 465 °C and t_q equal to 5 s.

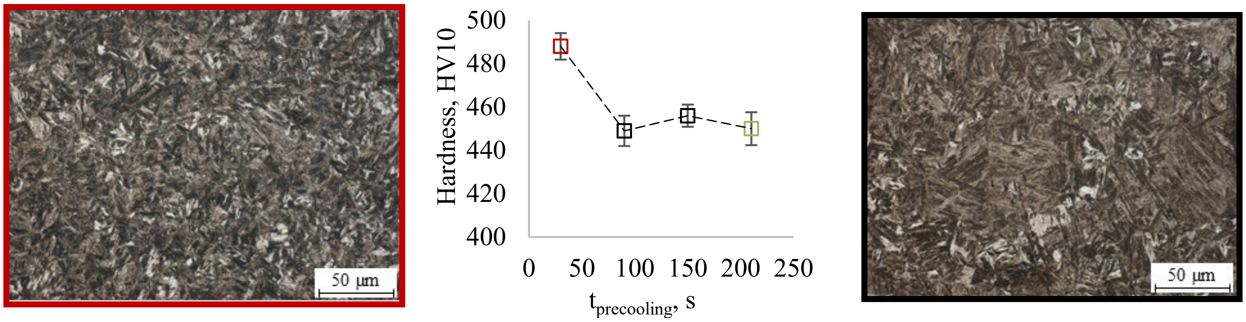

Fig. 9. Experimental hardness values as the $t_{precooling}$ varies referred to the resistant area obtained with IPC technology and micrographs (500 X) corresponding to the thermal cycles for $t_{precooling}$ equal to 30 s (image on the left) and $t_{precooling}$ equal to 210 s (image on the right).

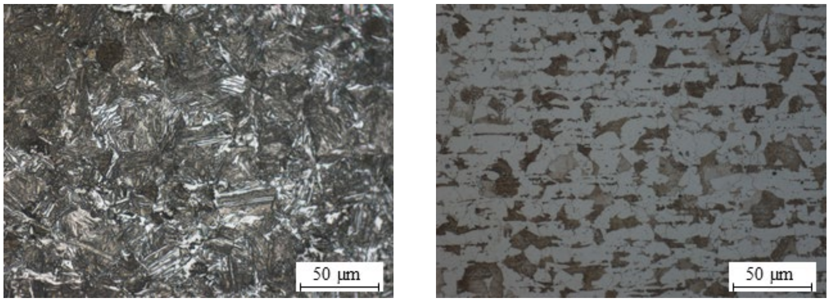

(a) (b)

Fig. 10. Micrographs (500X) corresponding to the thermal cycles of the ductile area for (a) $t_{precooling}$ equal to 30 s and (b) $t_{precooling}$ equal to 210 s.

In the ductile area obtained with the IPC technology, the metallographic analyses confirm the predictions of FE simulations. As an example, Fig. 10 shows the microstructure obtained for $T_{preccoling}$ = 600 °C both for $t_{precooling}$ = 30 s (Fig. 10a) and $t_{precooling}$ = 210 s (Fig. 10b). A mixed microstructure is observed in Fig. 10a, whereas a ferritic-pearlitic microstructure is observed in Fig. 10b, as predicted from numerical results summarised in Fig. 6.

With the aim of optimizing the TTT technology to obtain components with tailored properties, the results described so far allow to state that the optimal condition can be achieved by imposing a temperature of the heated tools of 465 °C and a quenching time equal to 5 s. These values guarantee at the same time low energy consumption, short process cycle time and completely bainitic microstructure in ductile areas and martensitic microstructure in resistant areas.

For the IPC technology, the optimal condition could be achieved by cooling down to a temperature of 600 °C in a time of 30 s the areas that are desired to be ductile. These process parameter values are optimal because a $T_{precooling}$ equal to 600 °C guarantees the maximum softening in ductile areas and a $t_{precooling}$ equal to 30 s avoids grain growth phenomenon in the resistant area.

After physical simulation tests, the specimens were subjected to tensile tests with the aim of comparing the ultimate tensile strength and the fracture deformability (strain at break) between the ductile zone obtained with the TTT technology and the one obtained with the IPC technology. Fig. 11 compares the engineering stress-strain curve of the TTT technology in the optimal condition (T_q465°C-t_q5s) with the IPC technology curves both in the optimal condition ($T_{precooling}$600°C-$t_{precooling}$30s) and in the maximum softening ($T_{precooling}$600°C-$t_{precooling}$210s). The deformations shown in Fig. 11 were obtained locally (at the breaking point) by means of the DIC system.

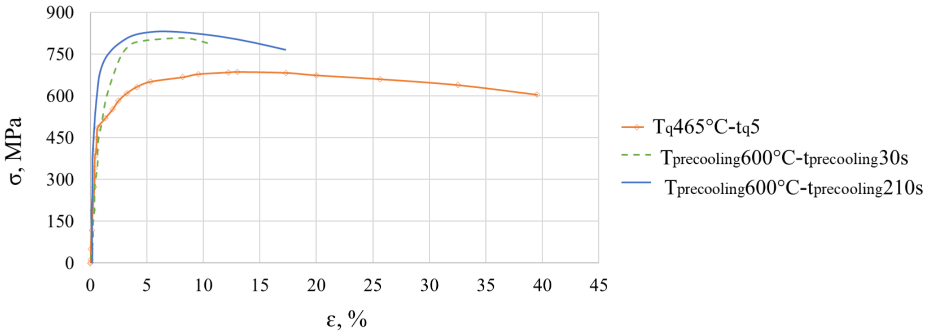

Fig. 11. Engineering stress-strain curves of (i) the TTT technology in the optimal condition, (ii) the IPC technology in the optimal condition and (iii) the IPC technology in the maximum softening condition.

From the comparison of the tensile testing curves in optimal conditions it can be observed that the TTT technology guarantees a greater fracture deformability in ductile regions, although the ultimate tensile strength is comparable. However, the greatest fracture deformability is reached during IPC process in the condition of maximum softening.

Conclusions

This work compared two tailored technologies for press hardening process, namely TTT and IPC for guaranteeing on the same component a resistant area with high strength and a ductile area with high fracture deformability. In TTT technology the ductile region (mainly bainitic) is obtained by increasing the heated tool temperature and the quenching time. However, to optimize the process, values of process parameters were chosen to ensure at the same time a good level of softening, low cycle times (low t_q) and low energy consumption (low T_q). In IPC technology, on the other hand, the ductile region (mainly ferritic-pearlitic) is obtained by increasing the time taken in the tempering station and lowering the temperature to which the blank drops in correspondence with the ductile regions. However, with this study was observed that an increase in $t_{precooling}$ leads to the problem of martensitic grain growth in the resistant region. Therefore, the optimal values of the process parameters were chosen in order to avoid this problem and ensure a good softening on the ductile part.

Comparing the conditions of maximum softening, the IPC technology guarantees a 40% lower hardness and a fracture deformability about double compared to the TTT technology. In terms of optimal conditions, the experimental plan shows that greater fracture deformability is reached with TTT technology. However, future work intends to investigate precooling times between 30 s and 90 s, which could guarantees higher softening in the soft zone and no grain growth problems in the hard zone.

Acknowledgments

The authors are grateful to PNRR - Spoke 11 (Innovative Materials and Lightweighting) project for funding this research and the Italian Ministry of University and Research that partly supported this research under the Programme “Department of Excellence” Legge 232/2016 (Grant No. CUP - D93C23000100001)”.

References

[1] Billur, Eren. "Hot stamping of ultra high-strength steels." From a technological and business perspective. Cham (2019). https://doi.org/10.1007/978-3-319-98870-2

[2] Neugebauer, R., et al. "Press hardening-An innovative and challenging technology." Archives of civil and mechanical engineering 12 (2012): 113-118. https://doi.org/10.1016/j.acme.2012.04.013

[3] Boretti, Alberto. "Plug-in hybrid electric vehicles are better than battery electric vehicles to reduce CO2 emissions until 2030." International Journal of Energy Research 46.14 (2022): 20136-20145. https://doi.org/10.1002/er.8313

[4] Merklein, Marion, et al. "Hot stamping of boron steel sheets with tailored properties: A review." Journal of materials processing technology 228 (2016): 11-24. https://doi.org/10.1016/j.jmatprotec.2015.09.023

[5] Cheng, Wei, et al. "A process-performance coupled design method for hot-stamped tailor rolled blank structure." Thin-Walled Structures 140 (2019): 132-143. https://doi.org/10.1016/j.tws.2019.03.037

[6] Samadian, Pedram, et al. "Fracture response in hot-stamped tailor-welded blanks of Ductibor® 500-AS and Usibor® 1500-AS: experiments and modelling." Engineering Fracture Mechanics 253 (2021): 107864. https://doi.org/10.1016/j.engfracmech.2021.107864

[7] Mori, Ken-ichiro, et al. "Combined process of hot stamping and mechanical joining for producing ultra-high strength steel patchwork components." Journal of Manufacturing Processes 59 (2020): 444-455. https://doi.org/10.1016/j.jmapro.2020.10.025

[8] Harrer, T., and M. Schäfer. "Laser softening of press hardened steel for novel automotive parts." Advanced High Strength Steel and Press Hardening: Proceedings of the 4th International Conference on Advanced High Strength Steel and Press Hardening (ICHSU2018). 2019. https://doi.org/10.1142/9789813277984_0079

[9] Palmieri, Maria Emanuela, Francesco Rocco Galetta, and Luigi Tricarico. "Study of Tailored Hot Stamping Process on Advanced High-Strength Steels." Journal of Manufacturing and Materials Processing 6.1 (2022): 11. https://doi.org/10.3390/jmmp6010011

[10] Information on https://formingworld.com/hotforming-tailored-temporing-methodologies/, accessed October 2022.

[11] Palmieri, Maria Emanuela, et al. "Analysis of transition zone on a hot-stamped part with tailored tool tempering approach by numerical and physical simulation." steel research international https://doi.org/10.1002/srin.202200665. https://doi.org/10.1002/srin.202200665

[12] Information on https://www.aptgroup.com/company/news/apt-launching-temperbox%C2%AE-new-cycle-time-neutral-production-solution-enables-tailored, accessed February 2023.

[13] Palmieri, Maria Emanuela, and Luigi Tricarico. "Numerical-experimental study of a tailored press-hardening technology with intermediate pre-cooling to manufacture an automotive component in advanced high strength steel." Sheet Metal 2023 25 (2023): 447. https://doi.org/10.21741/9781644902417-55